

Pulse compression and supercontinuum at different powers of femtosecond pulses in water

Feng Xu (徐 凤)^{1,2}, Jiansheng Liu (刘建胜)¹, Ruxin Li (李儒新)¹, and Zhizhan Xu (徐至展)¹

¹State Key Laboratory of High Field Laser Physics, Shanghai Institute of Optics and Fine Mechanics, Chinese Academy of Sciences, Shanghai 201800

²Graduate School of the Chinese Academy of Sciences, Beijing 100039

Received February 27, 2007

Propagation of femtosecond light pulses in water is investigated. By changing input power from slightly above to highly above threshold for self-focusing, it is shown that either group velocity dispersion (GVD) or multi-photon ionization (MPI) and multi-photon absorption (MPA) may arrest the collapse. When MPI and MPA dominate the propagation, the pulse can be self-compressed to a few optical cycles. In spectral domain, MPI alone induces a strong blue shift. MPA can restrain this strong blue shift.

OCIS codes: 320.2250, 320.5520, 190.7110, 140.0140.

Pulse compression has often been achieved relying on low-order nonlinearities (e.g., self-phase modulation (SPM)) to promote the desired spectral broadening. This occurs only for laser peak intensity well below the threshold for multi-photon ionization (MPI). However, nowadays laser sources accessing terawatt powers could produce energetic pulses above the millijoule level while keeping a short duration of femtosecond level. When a femtosecond pulse propagates through transparent media with the beam power exceeding the critical power for collapse, the phenomenon of filamentation occurs. The filamentation of ultrashort laser pulses propagating in matter has become a topic of intense research for more than a decade. With the high intensities reached in the filamentation, several nonlinear phenomena, e.g., multi-photon absorption (MPA), plasma formation, saturable nonlinear response, stimulated Raman scattering, etc., occur in addition to the optical Kerr effect. Besides, the filament regime is enriched by such peculiar phenomena as pulse splitting, self-steepening, shock formation, supercontinuum generation and conical emission^[1]. Plasma formation of filamentation in gases is known to us that it not only arrests the collapse, but also compresses and splits the temporal shape of the pulse^[2]. However, femtosecond pulse compression and supercontinuum in liquids has not been studied in detail. In this paper, we simulate femtosecond pulses propagating in water at different input powers from slightly above to highly above critical power. MPI can compress the pulse to a few optical cycles and induces a strong blue shift. MPA restrains this strong blue shift.

The theoretical model for pulse propagation in transparent media is based on an extended nonlinear Schrödinger (NLS) equation governing the slowly varying envelope of the light electric field, coupled to an evolution equation for the electron density generated by MPI^[3,4]. Assuming propagation along the z axis, the complex scalar envelope $\varepsilon(r, t, z)$ of the electric field and the electron density ρ of the excited plasma in a reference frame moving at the group velocity v_g evolve as

$$i\partial_z\varepsilon = -\frac{1}{2k}T^{-1}(\Delta_\perp\varepsilon) + \frac{k''}{2}\partial_t^2\varepsilon - k_0n_2T(|\varepsilon|^2\varepsilon)$$

$$+ \frac{k_0}{2n_0\rho_c}T^{-1}(\rho\varepsilon) - i\frac{\beta^{(K)}}{2}|\varepsilon|^{2K-2}\varepsilon, \quad (1)$$

$$\partial_t\rho = \frac{\beta^{(K)}}{K\hbar\omega_0}(1 - \rho/\rho_{\text{at}})|\varepsilon|^{2K}, \quad \rho \ll \rho_{\text{at}}, \quad (2)$$

where t refers to the retarded time variable $t - z/v_g$. The right hand side terms of Eq. (1) describe transverse diffraction, group velocity dispersion (GVD), nonlinear self-focusing related to the Kerr response of the material, defocusing due to the electron plasma, and MPA involving K photons, respectively. The laser field is characterized by the linear carrier frequency ω_0 and central wave number $k(\omega_0) = n_0k_0 = n_0\omega_0/c$ with the linear index of the medium n_0 ; the quantity k'' controls the magnitude and sign of the GVD, with $k'' > 0$ corresponding to normal dispersion and $k'' < 0$ to anomalous dispersion; n_2 is the nonlinear refraction index of the media. $\rho_c = \varepsilon_0m_e\omega_0^2/e^2$ denotes the critical plasma density beyond which the laser pulse no longer propagates (e and m_e are the electron charge and mass; ε_0 is the electric permittivity in vacuum). ρ_{at} is the density of neutral atoms. $\beta^{(K)} = K\hbar\omega_0\rho_{\text{at}}\sigma_K$ is the nonlinear coefficient for K -photon absorption with MPI coefficient σ_K , where K corresponds to the minimum number of photons with energy $\hbar\omega_0$ required for liberating an electron from a medium with ionization energy U_i , $K = \text{mod}(U_i/\hbar\omega_0) + 1$. Self-steepening effects are modelled by the operator $T = 1 + (i/\omega_0)\partial_t$ in front of the cubic nonlinearity, and space-time focusing is taken into account with T^{-1} in front of the transverse Laplacian operator.

Equation (1) is solved in axially symmetric geometry by means of a Fourier spectral decomposition in time and a standard Crank-Nicholson scheme in space. Equation (2) is solved by a Runge-Kutta method.

We assume the input field as a spatio-temporal Gaussian profile with a transverse waist $w_0 = 75 \mu\text{m}$ and pulse duration $t_p = 130$ fs,

$$\varepsilon(r_\perp, t, 0) = \sqrt{2P_{\text{in}}/\pi w_0^2} e^{-r^2/w_0^2 - t^2/t_p^2}, \quad (3)$$

where $P_{\text{in}} = \sqrt{2/\pi}E_{\text{in}}/t_p$ denotes the input power, and

the central wavelength of the laser pulse is $\lambda_0 = 800$ nm. The density of neutral atoms is taken as $\rho_{\text{at}} = 6.68 \times 10^{22}$ cm^{-3} . GVD coefficient takes the value $k'' = 248$ fs^2/cm . The refraction index $n_0 = 1.334$ and $n_2 = 4.1 \times 10^{-16}$ cm^2/W . Band-to-band transitions are induced in water with the gap potential $U_i = 6.5$ eV, yielding the number of photons $K = 5$ required for ionization. The MPI coefficient reads as $\sigma_K = 1.2 \times 10^{-52}$ $\text{s}^{-1}\text{cm}^{10}\text{W}^{-5}$ (which corresponds to $\beta_k = 1 \times 10^{-47}$ cm^7W^{-4}). In this letter we mainly aim at comparing the effects of different input powers, so we simply take $T = T^{-1} = 1$ for all simulations.

We start with considering $E_{\text{in}} = 0.35$ μJ , corresponding to an input power $P_{\text{in}} = 1.17P_{\text{cr}}$. The numerical simulation result for Eqs. (1) and (2) shows that the arrest of collapse is not promoted by MPI since generated electron density never exceeds 10^{12} cm^{-3} , and the peak intensity remains limited to $I_{\text{max}} < 7 \times 10^{10}$ W/cm^2 . Compared with the case in gases^[2], here the pulse begins to split slightly only when the peak intensity is very low, see the solid line in Fig. 1(a). This is due to that compared with gases the nonlinear index coefficient and the dispersive coefficient in water are very large, so pulse dynamic is different from that in gases. In this case the pulse is compressed by self-focusing and can be compressed to about 90 fs at its minimum width (see Fig. 1(a)).

As the input energy is increased to 1.0 μJ , the power ratio increases and the self-focusing dynamic overcomes GVD to the benefit of plasma formation. In this case, the pulse undergoes strong self-focusing, so the peak intensity of the pulse increases a lot. MPI mainly defocuses the trailing portion of the pulse, at this portion much energy is diverged into the outer part (reservoir) of beam. So the on-axis pulse becomes asymmetric at first. On further propagation, at the trailing part, MPI cannot counteract the effect of ever present self-focusing. The beam at the trailing edge regains power and self-focuses for the second time, resulting in the pulse splitting on axis. Figure 1(b) demonstrates this process. At $z = 1.40$ cm, the two sub-pulses can be respectively compressed to about 20 fs, a few optical cycles ($\tau_{\text{oc}} = \lambda_0/c$).

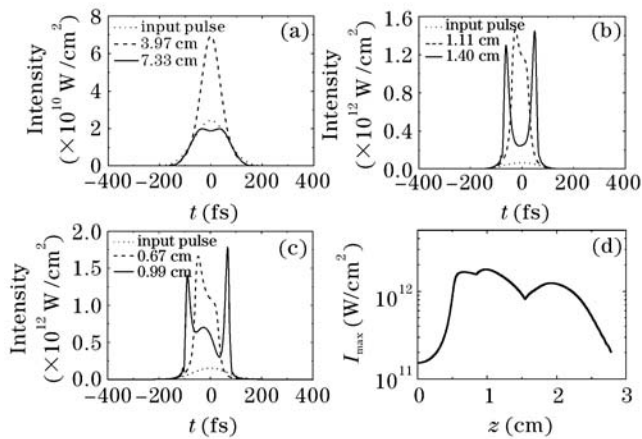


Fig. 1. (a)—(c) On-axis temporal profiles of the pulse intensity at different propagation distances for 800-nm pulse ($w_0 = 75$ μm , $t_p = 130$ fs) at input energy E_{in} of (a) 0.35, (b) 1.0, and (c) 2.2 μJ . (d) Evolution of peak intensity for 800-nm pulse at $E_{\text{in}} = 2.2$ μJ ($w_0 = 75$ μm , $t_p = 130$ fs).

For a comparison, we also simulate an input energy of 2.2 μJ . Figure 1(c) shows the on-axis temporal profiles at different propagation distances. This time the pulse self-focuses faster and the plasma channel lasts longer. But the peak intensity and maximum electron density of the plasma channel increase a little compared with the case of 1.0- μJ input pulse energy. This is because MPI and MPA affect much stronger as the intensity increases a little, preventing the plasma channel intensity from further increasing. Figure 1(d) demonstrates the evolution of peak intensity along the propagation. It indicates that the compressed pulse can propagate near a Rayleigh length ($z_R = \pi n_0 w_0^2 / \lambda_0 = 2.9$ cm).

The interaction of the high intensity in the self-focusing regions with the neutral media and with the plasma results in the modulation of the phase of the pulse, i.e., SPM. The consequence is spectral broadening towards both the red and the blue sides; i.e., supercontinuum generation. The spectra corresponding to Figs. 1(a)—(c) are shown in Fig. 2. In Fig. 2(a), it can be seen that the spectrum undergoes both red and blue shifts. As the input power is only slightly above critical value and plasma does not have the effect, the broadening is symmetric and small. Besides, the spectrum changes little along the propagation.

In the case of input energy of 1.0 μJ (Fig. 2(b)), SPM broadens the spectrum symmetrically at the beginning. When plasma begins to have the effect, a relatively strong blue shift emerges. However, after the pulse undergoes splitting through optical Kerr effect and MPI, a strong spectral broadening to both red and blue sides occurs, see the solid line in Fig. 2(b). In Fig. 2(c), as the input energy is much higher compared with Fig. 2(b), the broadening is stronger.

In order to see the plasma action on spectra, we simulate Eqs. (1) and (2) without MPA ($T = T^{-1} = 1$, $E_{\text{in}} = 2.2$ μJ), shown in Fig. 2(d). Very strong blue shift always presents over the filament. This can be explained as follows. To our knowledge, the front part of the pulse contributes principally to red shift; the back part of the pulse would lead to a blue shift. Besides, SPM in an optical medium is caused by the temporal variation of the refractive index. At the trailing edge, the pulse would

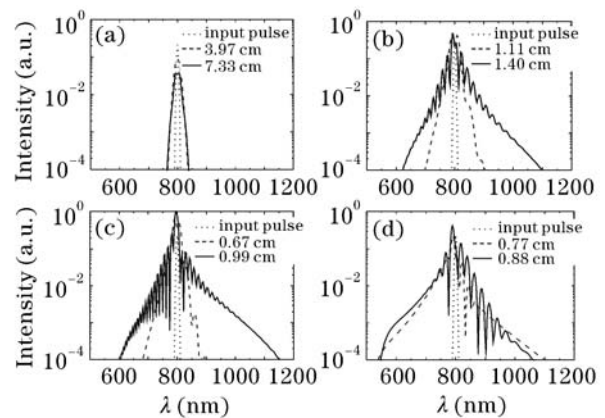


Fig. 2. (a)—(c) Power spectra at different propagation distances for 800-nm pulse ($w_0 = 75$ μm , $t_p = 130$ fs) at input energy E_{in} of (a) 0.35, (b) 1.0, and (c) 2.2 μJ . (d) Spectra at $E_{\text{in}} = 2.2$ μJ without MPA.

propagate at a velocity c/n where $n = n_0 + \Delta n_{\text{Kerr}} - \Delta n_{\text{p}}$, n is the total index of the refraction, n_0 , Δn_{Kerr} and Δn_{p} are the indices of the refraction of the neutral water, the nonlinear Kerr index, and the index of the plasma, respectively^[5,6]. At the trailing part, the intensity is weaker and the plasma density is higher compared with the center of the pulse. Hence n decreases, i.e., this trailing part will propagate faster than these with earlier t with the result of a shock wave formation. SPM is proportional to the derivative of this part of the pulse; thus a relatively large blue shift occurs.

Comparing Figs. 2(c) and (d), it can be found that when MPA is taken into account, the spectra broaden to both red and blue sides at the post collapse region. That means MPA can damp the strong blue shift induced by MPI.

In conclusion, the propagation of femtosecond laser pulses at different pulse powers in water is simulated using the standard model of NLS equation. GVD or MPI and MPA may arrest the collapse according to the input power. When the power is high enough for MPI to have the effect, the pulse can be self-compressed to a few optical cycles. In spectral domain, the broadening is

symmetric before MPI plays a role. Then MPI can induce a strong blue shift, however, MPA would damp this effect.

This work was supported by the Chinese National Major Basic Research Development Program (973 Program), and the National Natural Science Foundation of China (No. 10674145). F. Xu's e-mail address is xf_aurora@mail.siom.ac.cn.

References

1. A. Gaeta, *Science* **301**, 54 (2003).
2. S. Champeaux and L. Bergé, *Phys. Rev. E* **68**, 066603 (2003).
3. M. Mlejnek, E. M. Wright, and J. M. Moloney, *Phys. Rev. E* **58**, 4903 (1998).
4. M. D. Feit and J. A. Fleck, *Appl. Phys. Lett.* **24**, 169 (1974).
5. S. L. Chin, S. A. Hosseini, W. Liu, Q. Luo, F. Théberge, N. Aozbek, A. Becker, V. P. Kandidov, O. G. Kosareva, and H. Schroeder, *Can. J. Phys.* **83**, 863 (2005).
6. J. Liu, R. Li, and Z. Xu, *Phys. Rev. A* **74**, 043801 (2006).